2 Heaviside Operational Calculus and Electromagnetic Image Theory

I.V. Lindell

Helsinki University of Technology, PO Box 3000, FIN-02015HUT, Espoo, Finland

Abstract. The image principle in electromagnetics replaces a physical structure by an equivalent source, the image of the primary source. The number of structures with analytic image expressions is limited but increasing. In finding new image expressions, the Heaviside operational calculus can be applied by first transforming the three-dimensional problem to one concerning transmission lines. The image problem can be reduced to the compact form in terms of a pseudo-differential operator applied to the original source function. To interprete the result in terms of computable functions, approximations can be done at this stage. As a simple example of the theory the interface of two isotropic media with smooth or slightly rough interface is considered. A table of operational formulas is given as an appendix.

1 The Image Principle

The image principle gives a simple method to treat electromagnetic problems involving interfaces of material media [1,2] by replacing the structure behind the interface by an equivalent image source in a homogeneous medium. Most probably the first definition of the image concept in electricity or magnetism was given by William Thomson (later Lord Kelvin) in 1849 [3]:

> The term *Electrical Images*, which will be applied to the imaginary electrical points or groups of electrical points, is suggested by the received language of Optics; and the close analogy of optical images will, it is hoped, be considered as a sufficient justification for the introduction of a new and extremely convenient mode of expression into the Theory of Electricity.

Formulating an electromagnetic problem involving a physical structure in terms of an image source can be compared to working with the Green function associated with the boundary-value problem. The image principle may well be the simpler choice because in many structures it can be expressed in closed form while the Green function cannot. Actually, the Green function can always be written in the form of an integral of the image source. Because the image source is a quasi-physical concept, physical intuition can help in the computation of fields. In fact, fields arise from image sources in the same way as they do from physical sources. Also, image sources can be approximated like the physical sources to simplify the computation, even if the image source might exist in complex space. Further, image sources can take the role of unknown in integral equations.

F. Moreno and F. González (Eds.): Lectures 1998, LNP 534, pp. 23–39, 2000.

Simple Example

To keep equations simple, let us consider a scattering example from electrostatics. Assume a static charge distribution $\varrho_o(\mathbf{r})$ and a dielectric scatterer of permittivity $\epsilon(\mathbf{r}) = \epsilon_o\epsilon_r(\mathbf{r})$ in air above a layered planar structure $z < 0$. The potential scattered by the obstacle can be computed after solving the dielectric polarization distribution within the obstacle. This can be done numerically through an integral equation for the equivalent polarization charge density $\varrho_p(\mathbf{r})$, which can be defined by writing the Gaussian law in inhomogeneous dielectric medium as

$$\nabla \cdot \mathbf{D}(\mathbf{r}) = \nabla \cdot [\epsilon(\mathbf{r})\mathbf{E}(\mathbf{r})] = \varrho_o(\mathbf{r}). \tag{1}$$

If the obstacle is replaced by the equivalent polarization charge in air, we can write

$$\nabla \cdot [\epsilon_o\mathbf{E}(\mathbf{r})] = \varrho_o(\mathbf{r}) + \varrho_p(\mathbf{r}). \tag{2}$$

From comparison, the equivalent charge becomes

$$\varrho_p(\mathbf{r}) = -\epsilon_o\nabla \cdot [(\epsilon_r(\mathbf{r}) - 1)\mathbf{E}(\mathbf{r})], \tag{3}$$

which is nonzero only inside the scatterer where $\epsilon_r(\mathbf{r}) \neq 1$.

Now let us consider two possible ways of forming the integral equation. First, assuming that the Green function $G(\mathbf{r}|\mathbf{r}')$, i.e., the potential at $\mathbf{r}$ due to a normalized point source at $\mathbf{r}'$ in the presence of the planar structure is known, the potential from any charge distribution $\varrho(\mathbf{r}')$ can be expressed as the integral

$$\phi(\mathbf{r}) = \int G(\mathbf{r}|\mathbf{r}')\frac{\varrho(\mathbf{r}')}{\epsilon_o}dV'. \tag{4}$$

When computing values for the potential inside the source, the singularity of the Green function in the integral must be taken into account in a proper way.

The potential inside the obstacle is due to the original source (incident potential ϕ_i) and the equivalent polarization source (scattered potential ϕ_s), both in the presence of the structure:

$$\phi(\mathbf{r}) = \phi_i(\mathbf{r}) + \phi_s(\mathbf{r}), \tag{5}$$

$$\phi_i(\mathbf{r}) = \int G(\mathbf{r}|\mathbf{r}')\frac{\varrho_o(\mathbf{r}')}{\epsilon_o}dV', \qquad \phi_s(\mathbf{r}) = \int G(\mathbf{r}|\mathbf{r}')\frac{\varrho_p(\mathbf{r}')}{\epsilon_o}dV'. \tag{6}$$

The incident potential can be considered as a known function. The scattered potential involves an unknown source ϱ_p, which depends on the unknown total potential $\phi(\mathbf{r})$. This gives rise to an integral equation for the total potential:

$$\phi(\mathbf{r}) = \phi_i(\mathbf{r}) + \int G(\mathbf{r}|\mathbf{r}')\nabla' \cdot [(\epsilon_r(\mathbf{r}') - 1)\nabla'\phi(\mathbf{r}')]dV', \tag{7}$$

which can be solved numerically if only the Green function $G(\mathbf{r}|\mathbf{r}')$ happens to be known. Finding the Green function $G(\mathbf{r}|\mathbf{r}')$ may well be the most difficult task of the problem and normally leads to a numerical analysis of another integral equation.

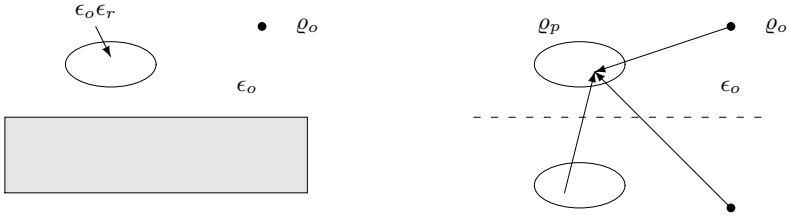

Fig. 1. Original charge ϱ_o and a scatterer above a planar structure. The integral equation for the potential in the equivalent polarization charge ϱ_p is obtained with the aid of images of the original charge and the unknown polarization charge. The figure is drawn in simplified form, because, in general, the image of a point source is not a simple point source.

In contrast, in the image formulation, only the free-space Green function $G_o(\mathbf{r} - \mathbf{r}') = 1/4\pi|\mathbf{r} - \mathbf{r}'|$ is needed. However, now the image for the general point charge above the planar structure must be known. The integral equation for the total potential inside the scatterer can be formed by replacing the planar structure through the images of the original charge distribution and the unknown polarization charge distribution, Fig. 1. Similar arguments apply to problems involving time-harmonic sources with vector sources and dyadic Green functions. It is thus of basic interest to find image expressions for the point source with respect to different structures.

2 Heaviside Calculus

Oliver Heaviside (1850-1925) constructed the modern electromagnetic theory in compact form [4] by introducing the vector notation simultaneously with J.W. Gibbs. In his analysis of electromagnetic equations he also used a form of operational calculus, which eventually led to the Laplace transform technique and to other operator methods [5,6]. In his calculus, Heaviside treated differential operators very much as ordinary numbers, which allowed him to apply simple rules of algebra to solving differential equation problems. In the following it will be demonstrated that the Heaviside operational calculus can be effectively applied to finding image solutions for electromagnetic problems by starting from transmission-line concepts.

The relation between the Laplace transform technique and operational calculus can be applied to define some operational formulas readily applicable to the image analysis. The definition of the Laplace transform $f(p) \to F(q)$

$$F(q) = \int_0^\infty f(p) \exp(-pq) dp \tag{8}$$

leads through substitution $q = \partial_z = \partial/\partial z$ to a (pseudo-differential) operator $F(\partial_z)$, which operating on the delta function $\delta(z - z_o)$ gives us the rule

$$F(\partial_z)\delta(z - z_o) = \int_0^\infty f(p) \exp(-p\partial_z)\delta(z - z_o) dp = f(z - z_o)\theta(z - z_o). \tag{9}$$

Here we have applied the Taylor expansion of an exponential function and the shifting rule,

$$\exp(-pq) = \sum_{n=0}^{\infty} \frac{(-p)^n}{n!} q^n, \qquad \exp(-p\partial_z) f(z) = f(z - p). \tag{10}$$

$\theta(z)$ denotes the Heaviside unit step function

$$\theta(z) = 0, \quad z < 0, \qquad \theta(z) = 1, \quad z \geq 0. \tag{11}$$

Equation (9) forms the basis of the Heaviside operator method applied here. Typically, the image of a point source is obtained in the form of an operator $F(\partial_z)$ operating on the delta function. The task is to find the function $f(z)$, which defines the image in terms of a computable function. Applying existing tables of Laplace transforms, we can write a table of pseudo-differential operators operating on the delta function. A short one is given as an Appendix.

3 Transmission-Line Theory

Transmission-Line Equations

To solve the original three-dimensional problem, it is often necessary to reduce the dimension from three to one, for example, by making a Fourier transformation in two dimensions. After solving the problem in one dimension, the solution can be transformed back to three dimensions. The Maxwell equations then become transmission-line equations and the electromagnetic field vectors can be replaced by voltage $U(z)$ and current $I(z)$ functions:

$$\partial_z U(z) = -j\beta Z I(z) + u(z), \tag{12}$$

$$\partial_z I(z) = -j\beta Y U(z) + i(z). \tag{13}$$

Here, $u(z)$ and $i(z)$ denote the distributed voltage and current source functions. β is the (complex) propagation constant and $Z = 1/Y$ the line impedance and they are assumed constant, corresponding to a homogeneous 3D space. The second-order transmission-line equations are obtained after elimination as

$$(\partial_z^2 + \beta^2)U(z) = \partial_z u(z) - j\beta Z i(z), \tag{14}$$

$$(\partial_z^2 + \beta^2)I(z) = \partial_z i(z) - j\beta Y i(z). \tag{15}$$

In some problems transmission-line equations more general than (12), (13) are needed with different line parameters β, Z for waves traveling to opposite directions along the line [8].

A combined voltage-current point source at $z = z_o$ on the transmission line

$$u^i(z) = U_o\delta(z - z_o), \quad i^i(z) = I_o\delta(z - z_o), \tag{16}$$

produces incident voltage and current functions

$$U^i(z) = \frac{1}{2}[\mathrm{sgn}(z - z_o)U_o + ZI_o]\exp(-j\beta|z - z_o|), \tag{17}$$

$$I^i(z) = \frac{1}{2}[\mathrm{sgn}(z - z_o)I_o + YU_o]\exp(-j\beta|z - z_o|). \tag{18}$$

Inserting these expressions in (14) and (15), their validity can be checked.

Reflection from Load Impedance

Let us consider a half-infinite homogeneous transmission line $z < 0$ terminated by a load impedance Z_L at $z = 0$, Fig. 2. Assuming a point source at $z = z_o < 0$, which creates the incident wave (17), (18), the reflected voltage and current waves can be expressed as

$$U^r(z) = RU^i(0)exp(j\beta z) = \frac{R}{2}(U_o + ZI_o)\exp(j\beta z_o)\exp(j\beta z), \tag{19}$$

$$I^r(z) = -YU^r(z) = -\frac{R}{2}(I_o + YU_o)\exp(j\beta z_o)\exp(j\beta z). \tag{20}$$

The load impedance Z_L may represent a physical structure (an inhomogeneous transmission line, for example) existing in the region $z > 0$. In the

general case, the reflection coefficient is a function of the propagation constant, $R = R(\beta)$. In the expression of the reflected voltage it can be replaced by an operator $R(-j\partial_z)$ operating on an exponential function

$$U^r(z) = R(\beta)U^i(0)\exp(j\beta z) = U^i(0)R(-j\partial_z)\exp(j\beta z)$$

$$= \frac{R}{2}(U_o + ZI_o)\exp(j\beta(z+z_o)) = R(-j\partial_z)U^i(-z). \tag{21}$$

If $R(\beta)$ is a polynomial function, $R(-j\partial_z)$ is a differential operator, otherwise it is a pseudo-differential operator. The form of the reflection-coefficient function is obtained from the boundary condition as

$$U^i(0) + U^r(0) = Z_L[I^i(0) + I^r(0)] \quad \Rightarrow \quad R = \frac{Z_L - Z}{Z_L + Z}. \tag{22}$$

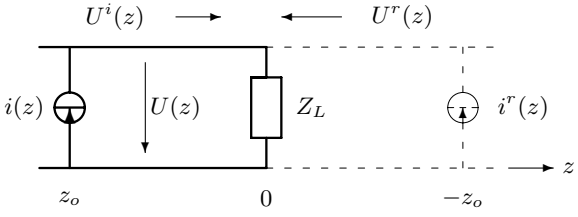

Fig. 2. Reflection image i^r of a current source i at $z_o < 0$ lies on the extension of the transmission line at $-z_o$. It gives the voltage $U^r(z)$ reflected from the load impedance Z_L.

Image Sources

Let us now replace the load impedance by finding the image sources in the extension $z > 0$ of the homogeneous transmission line which give the same reflected wave (21) in the region $z < 0$, Fig.2. The source of the reflected voltage $U^r(z)$ can be obtained in the same way as the source of the incident wave in (14), by applying the operator $\partial_z^2 + \beta^2$ on (21) and identifying the right-hand source terms:

$$(\partial_z^2 + \beta^2)U^r(z) = R(-j\partial_z)(\partial_z^2 + \beta^2)U^i(-z)$$

$$= R(-j\partial_z)[-\partial_z u^i(-z) - j\beta Z i^i(-z)]. \tag{23}$$

Denoting the reflection images by $u^r(z)$ and $i^r(z)$ and substituting the original sources, we have

$$\partial_z u^r(z) - j\beta Z i^r(z) = R(-j\partial_z)[-\partial_z u^i(-z) - j\beta Z i^i(-z)], \tag{24}$$

from which we can identify the image sources as

$$u^r(z) = -R(-j\partial_z)u^i(-z), \quad i^r(z) = R(-j\partial_z)i^i(-z). \tag{25}$$

For the point sources (16) the images are

$$u^r(z) = -R(-j\partial_z)U_o\delta(z+z_o), \quad i^r(z) = R(-j\partial_z)I_o\delta(z+z_o). \tag{26}$$

The expressions (26) form the basis of the image method discussed here. In the simplest case when the reflection coefficient R does not depend on β, the reflection image consists of voltage and current generators at the image point $z = -z_o$ with the respective amplitudes $-RU_o$, RI_o.

4 Time-Harmonic Planar Problems

Let us consider problems involving a planar stratified structure, with material parameters depending on one coordinate z only. In this case, the one-dimensional image theory can be applied by making the Fourier transform in the xy plane, whence the problem becomes analogous to that of a transmission line [2].

Transmission-Line Analogy

The Fourier-transformed Maxwell equations are

$$\mathbf{u}_z \times \partial_z \mathbf{E} - j\mathbf{K} \times \mathbf{E} = -j\omega\mu\mathbf{H} - \mathbf{M}, \tag{27}$$

$$\mathbf{u}_z \times \partial_z \mathbf{H} - j\mathbf{K} \times \mathbf{H} = j\omega\epsilon\mathbf{E} + \mathbf{J}, \tag{28}$$

where the electric and magnetic fields $\mathbf{E}, \mathbf{H}$ and the electric and magnetic sources $\mathbf{J}, \mathbf{M}$ are functions of z and the two-dimensional Fourier variable $\mathbf{K}$. Equations (27), (28) can be represented as a coupled pair of transmission lines. The field components transverse to z give rise to two sets of voltage and current quantities

$$U_e = \frac{1}{K^2}\mathbf{K} \cdot \mathbf{E}, \quad I_e = \frac{1}{K^2}\mathbf{u}_z \times \mathbf{K} \cdot \mathbf{H}, \tag{29}$$

$$U_m = \frac{1}{K^2}\mathbf{u}_z \times \mathbf{K} \cdot \mathbf{E}, \quad I_m = -\frac{1}{K^2}\mathbf{K} \cdot \mathbf{H}, \tag{30}$$

and the transverse fields can be expressed as

$$\mathbf{E}_t = \mathbf{K}U_e + \mathbf{u}_z \times \mathbf{K}U_m, \tag{31}$$

$$-\mathbf{u}_z \times \mathbf{H} = \mathbf{K}I_e + \mathbf{u}_z \times \mathbf{K}I_m. \tag{32}$$

The two transmission lines are uncoupled in homogeneous space and obey the equations

$$(\partial_z^2 + \beta^2)U_{e,m}(z) = \partial_z u_{e,m}(z) - j\beta Z_{e,m} i_{e,m}(z), \tag{33}$$

$$(\partial_z^2 + \beta^2)I_{e,m}(z) = \partial_z i_{e,m}(z) - j\beta Y_{e,m} u_{e,m}(z), \tag{34}$$

where the source functions are

$$u_e(z) = -\frac{1}{K^2}\mathbf{u}_z \times \mathbf{K} \cdot \mathbf{M}(z) + \frac{1}{\omega\epsilon}\mathbf{u}_z \cdot \mathbf{J}(z), \qquad i_e(z) = -\frac{1}{K^2}\mathbf{K} \cdot \mathbf{J}(z), \tag{35}$$

$$i_m(z) = -\frac{1}{K^2}\mathbf{u}_z \times \mathbf{K} \cdot \mathbf{J}(z) - \frac{1}{\omega\mu}\mathbf{u}_z \cdot \mathbf{M}(z), \qquad u_m(z) = \frac{1}{K^2}\mathbf{K} \cdot \mathbf{M}(z). \tag{36}$$

The propagation factor is the same for both lines but the impedance is different:

$$\beta = \sqrt{k^2 - K^2}, \qquad k = \omega\sqrt{\mu\epsilon}, \tag{37}$$

$$Z_e = \frac{\beta}{\omega\epsilon} = \frac{\beta}{k}\eta, \qquad Z_m = \frac{\omega\mu}{\beta} = \frac{k}{\beta}\eta, \qquad \eta = \sqrt{\frac{\mu}{\epsilon}}. \tag{38}$$

When there is an interface of two media at $z = 0$, coupling may arise between the two lines, which can be represented by a coupling two-port network. This means for example that, a source in the e line may create image sources in both e and m lines. However, for an interface between two isotropic media, there is no such coupling and the lines can be understood as terminated by individual impedances Z_{Le} and Z_{Lm}.

Vertical Magnetic Dipole

As a simple example, let us consider a vertical magnetic current source (dipole) in the air (ϵ_o, μ_o) region $z < 0$, above a dielectric half space $(\epsilon_r\epsilon_o, \mu_o)$ in $z > 0$. Since i_m is the only source, only the m line exists and the subscript m will be omitted. The correponding reflection coefficient at the interface is

$$R(\beta_o) = \frac{Z_L - Z}{Z_L + Z} = -\frac{\beta - \beta_o}{\beta + \beta_o}. \tag{39}$$

The relation between the two propagation factors β, β_o is

$$\beta = \sqrt{k^2 - K^2} = \sqrt{k^2 - k_o^2 + k_o^2 - K^2} = \sqrt{\beta_o^2 - B^2}, \tag{40}$$

with

$$B = \sqrt{k_o^2 - k^2} = k_o\sqrt{1 - \epsilon_r}. \tag{41}$$

For perfectly electrically conducting (PEC) or perfectly magnetically conducting (PMC) surfaces corresponding respectively to $\epsilon_r = \infty$ and $\epsilon_r = 0$, we have $R = -1$ and $R = +1$ corresponding to short and open circuit at $z = 0$.

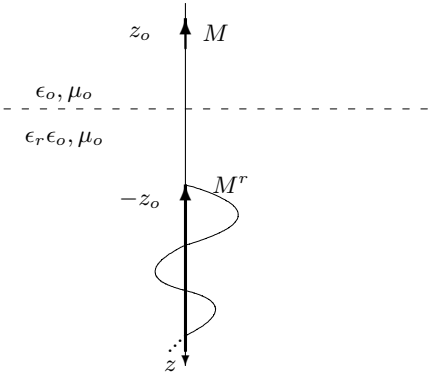

Fig. 3. The dielectric half space $z < 0$ can be replaced by the reflection image M^r of the original magnetic dipole M. The image consists of a magnetic dipole and a magnetic line current obeying Bessel function law.

The vertical magnetic dipole of moment M_oL corresponds to a current source in the transmission line:

$$\mathbf{M}(\mathbf{r}) = \mathbf{u}_z M_o L\delta(\mathbf{r} - \mathbf{u}_z z_o) \quad \Rightarrow \quad i(z) = I_o\delta(z - z_o), \quad I_o = -\frac{1}{\omega\mu_o}M_oL. \tag{42}$$

For the reflection image we now have from (26) the simple formal solution

$$i^r(z) = R(-j\partial_z)I_o\delta(z + z_o), \tag{43}$$

or, more explicitly,

$$i^r(z) = -I_o\frac{\sqrt{\partial_z^2 + B^2} - \partial_z}{\sqrt{\partial_z^2 + B^2} + \partial_z}\delta(z + z_o). \tag{44}$$

Invoking (73) for $n = 2$ from the Appendix, the solution can be expressed as

$$i^r(z) = -I_o \frac{2}{z} J_2(Bz)\theta(z). \tag{45}$$

Because the image does not depend on the Fourier variable $\mathbf{K}$, the corresponding vertical magnetic current source has $\delta(\boldsymbol{\rho}) = \delta(x)\delta(y)$ dependence,

$$\mathbf{M}^r(\mathbf{r}) = -\mathbf{u}_z \omega \mu_o i^r(z)\delta(\boldsymbol{\rho}) = -\mathbf{u}_z M_o L \frac{2}{z} J_2(Bz)\theta(z+z_o)\delta(\boldsymbol{\rho}). \tag{46}$$

Thus, the image is a magnetic line source extending from $z = -z_o > 0$ to ∞ obeying the Bessel function $J_2(Bz)$, Fig.3. The result (46) was previously obtained in [9,2] through a much more complicated analysis.

It must be noted that the image expression works well for real $\epsilon_r < 1$, ϵ_r being the ratio of the two permittivities. If $\epsilon_r > 1$, the coefficient B is imaginary and the Bessel function $J_2(Bz)$ diverges for real z. The same happens for complex ϵ_r. By assuming the image along a line in complex space as explained in [9,2], a useful converging image source is, however, obtained. A source in complex space can be applied numerically to compute fields in the physical space with the same ease as a source in real space. Because the Green function decays exponentially when the source lies in complex space, some computation time can be saved.

5 Slightly Rough Interface

As a second example, an extension of the previous one, let us consider the problem of two dielectric half spaces with a slightly rough planar interface, whose average coincides with the plane $z = 0$. The interface is defined by the height function $h(\boldsymbol{\rho})$, which is assumed to be a random variable obeying the Gaussian probability law,

$$P(h) = \frac{1}{\sigma\sqrt{2\pi}} \exp(-h^2/2\sigma^2). \tag{47}$$

The parameter σ is a measure of the rms surface height variation.

Reflection-Coefficient Method

Applying the well-known expression for the reflection coefficient corresponding to the coherent part of the reflected plane wave from a slightly rough surface, we can write [10,11]

$$R = R_s \exp(-2k_o^2\sigma^2 \cos^2\theta_i), \tag{48}$$

where θ_i is the angle of incidence. R_s denotes the reflection coefficient corresponding to a smooth surface ($\sigma = 0$), also a function of θ_i. For grazing

incidence $\theta_i \to \pi/2$, the reflection coefficient approaches that of the smooth surface.

Considering fields arising from a source above the interface, Fourier transformation again reduces the problem to one expanded in terms of plane waves. For each plane wave the reflection coefficient (48) can be applied in the form

$$R(\beta_o) = R_s(\beta_o)\exp(-2(k_o^2 - K^2)\sigma^2) = R_s(\beta_o)\exp(-2\beta_o^2\sigma^2). \tag{49}$$

The relation between the two-dimensional vector Fourier variable $\mathbf{K}$ and the angle of incidence defined by the unit vector $\mathbf{u}$ is

$$\mathbf{K} = \mathbf{u}k\sin\theta_i, \qquad \beta_o = \sqrt{k^2 - \mathbf{K}\cdot\mathbf{K}}. \tag{50}$$

After the Fourier transformation, the fields depend on one coordinate z only and the previous transmission-line analogy can be applied with β_o as the propagation constant.

Vertical Magnetic Dipole

Considering the vertical magnetic dipole source, the previous theory can now be applied with the reflection coefficient (48) replacing (39):

$$R(\beta_o) = R_s(\beta_o)\exp(-2\beta_1^2\sigma^2) = -\frac{\beta - \beta_o}{\beta + \beta_o}\exp(-2\beta_o^2\sigma^2). \tag{51}$$

Thus, the only difference in the resulting image is the extended reflection operator

$$\begin{aligned}\mathbf{M}^r(r) &= \mathbf{u}_z M_o L R(-j\partial_z)\delta(z + z_o)\delta(\boldsymbol{\rho}) \\ &= \mathbf{u}_z M_o L R_s(-j\partial_z)\exp(2\sigma^2\partial_z^2)\delta(z + z_o)\delta(\boldsymbol{\rho}).\end{aligned} \tag{52}$$

and the problem is to interpret the expression involving a product of two operators

$$R(-j\partial_z)\delta(z + z_o) = \exp(2\sigma^2\partial_z^2)R_s(-j\partial_z)\delta(z + z_o). \tag{53}$$

Extending the expression (9) to the product of two operators $F_1(\partial_z)$, $F_2(\partial_z)$ satisfying

$$F_i(\partial_z)\delta(z) = f_i(z)\theta(z), \qquad i = 1, 2, \tag{54}$$

leads to the following convolution rule:

$$F_1(\partial_z)F_2(\partial_z)\delta(z) = F_1(\partial_z)[f_2(z)\theta(z)] = \int_0^\infty f_1(p)\exp(-p\partial_z)[f_2(z)\theta(z)]dp$$

$$= \int_0^\infty f_1(p)[f_2(z-p)\theta(z-h)]dp = [f_1(z)\theta(z)] * [f_2(z)\theta(z)]. \tag{55}$$

Thus, the image of a rough dielectric interface can be expressed as the convolution of the images corresponding to the smooth dielectric interface and the rough PMC surface. The former was considered above.

Let us consider the image due to a rough perfect magnetic conductor (PMC) surface which is obtained as the limit $\epsilon_r \to 0$ of the dielectric interface. Because we now have $R_s = 1$, (53) reduces to

$$R(-j\partial_z)\delta(z+z_o) = \exp(2\sigma^2\partial_z^2)\delta(z+z_o). \tag{56}$$

The corresponding magnetic current image can be written as

$$\mathbf{M}^r(\mathbf{r}) = \mathbf{u}_z M_o L \exp(2\sigma^2\partial_z^2)\delta(z+z_o)\delta(\boldsymbol{\rho}). \tag{57}$$

To find the image function we invoke a result from [5] which cannot be found from Laplace transform tables,

$$\exp(\alpha\partial_z^2)\delta(z) = \frac{1}{\sqrt{2\pi\alpha}}\exp(-z^2/4\alpha). \tag{58}$$

This leads to

$$\mathbf{M}^r(\mathbf{r}) = \mathbf{u}_z \frac{M_o L}{\sqrt{8\pi}\sigma}\exp(-(z+z_o)^2/8\sigma^2)\delta(\boldsymbol{\rho}). \tag{59}$$

This represents a magnetic line current obeying the Gaussian distribution, with its maximum at the image point $z = -z_o$, Fig.4.

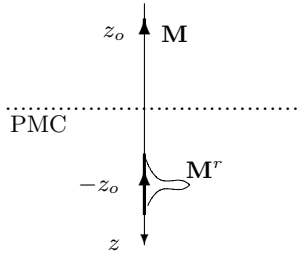

Fig. 4. Image of a vertical magnetic dipole above a slightly rough PMC plane is a magnetic line current broadened to a Gaussian pulse when the roughness of the surface obeys Gaussian statistics.

The image function corresponding to the rough dielectric interface can now be interpreted from (53) as the convolution

$$\exp(2\sigma^2\partial_z^2)R_s(j\partial_z)\delta(z) = -\frac{1}{\sqrt{2\pi}\sigma}\int_{-\infty}^{0}\exp(-(z'-z)^2/8\sigma^2)\frac{1}{z'}J_2(Bz')dz', \tag{60}$$

which gives a blurred specular image [12]. It does not seem possible to find a closed-form expression for this image function. Numerical values can, however, be easily computed from the convolution integral and stored in the computer memory for quick reuse in an integral equation solution process, for example. The image function $f(z)$ has properties similar to those of the specular image function.

The change in the amplitude of the coherent reflected wave due to the roughness of the surface can now be interpreted in terms of the image theory. When a point image becomes a line image of Gaussian distribution, the ensuing phase difference makes partial cancelation in the radiated field. This effect is most notable in the normal direction and disappears in the direction tangential to the interface.

The image principle described can be applied to a wide variety of problems involving a rough surface. For example, scattering from an object above a rough surface can be handled by replacing the object through an equivalent polarization source. Because of the approximative nature of the starting reflection coefficient (48), the image method has some limitations. Theoretically the image line extends from $z = -\infty$ to $z = +\infty$ and thus enters the wrong half space $z < 0$. However, because the roughness was assumed slight, the parameter σ is small, which means that the Gaussian distribution is very concentrated. Also, the plane-wave reflection approximation requires that the source height z_o be large enough so that surface waves are not excited. Because of these limitations, the image has a negligible value in the region $z < 0$.

6 Other Structures with Image Solutions

A number of other structures have been studied in the past, through various methods, for finding analytic expressions of the image function corresponding to the structure in question. It may suffice to mention some solved cases and refer to the literature for details. For planar structures, the microstrip geometry (dielectric slab above PEC plane) [13], the dielectric slab in air [14] and the uniaxial anisotropic hald space [15] have been treated for time-harmonic sources while the general anisotropic half space has been solved for electrostatic sources [16]. A solution with more general time dependence involving a noncausal current was found for the impulse source in [17]. Also, a slightly chiral half space has found an analytic solution [18].

The classical Kelvin's electrostatic image theory for a PEC sphere has been extended to the dielectric sphere [19], also solvable through the generalized asymmetric transmission-line concept [8]. The theory was extended to the layered sphere [20] and low-frequency time-harmonic sources [21]. Other solved non-planar geometries include the conducting half plane [22] and the conducting wedge [23] for time-harmonic sources and the dielectric wedge [24] for electrostatic sources as well as the conducting spheroid [25].

As mentioned in the introductory part, image expressions like those above can be readily applied to scattering problems, some examples of which are given in references [26–28].

Appendix: Table of Operations

Applying a table of Laplace transforms in, e.g., from [29], we can write a corresponding table for some pseudo-differential operators $F(\partial_z)$ operating on the delta function[1]:

$$F(\partial_z)\delta(z) = f(z)\theta(z).$$

$$\partial_z^{-n}\delta(z) = \frac{z^{n-1}}{(n-1)!}\theta(z), \tag{61}$$

$$\partial_z^{-1/2}\delta(z) = \frac{1}{\sqrt{\partial_z}}\delta(z) = \frac{1}{\sqrt{\pi z}}\theta(z), \tag{62}$$

$$\partial_z^{-3/2}\delta(z) = 2\sqrt{z/\pi}\theta(z), \tag{63}$$

$$\partial_z^{-\nu}\delta(z) = \frac{z^{\nu-1}}{\Gamma(\nu)}\theta(z), \quad \nu > 0, \tag{64}$$

$$\frac{1}{\partial_z + B}\delta(z) = \exp(-Bz)\theta(z), \tag{65}$$

$$\frac{\partial_z + B_1}{\partial_z + B_2}\delta(z) = \delta(z) + (B_1 - B_2)\exp(-B_2 z)\theta(z), \tag{66}$$

$$\frac{1}{(\partial_z + B)^2}\delta(z) = z\exp(-Bz)\theta(z), \tag{67}$$

[1] $n = 1, 2, 3, \cdots$ is an integer while ν may be any number.

$$\frac{1}{(\partial_z + B_1)(\partial_z + B_2)}\delta(z) = -\frac{\exp(-B_1 z) - \exp(-B_2 z)}{B_1 - B_2}\theta(z), \tag{68}$$

$$\frac{1}{\partial_z^2 + B^2}\delta(z) = \frac{1}{B}\sin(Bz)\theta(z), \tag{69}$$

$$(\sqrt{\partial_z + B_1} - \sqrt{\partial_z + B_2})\delta(z) = -\frac{1}{2\sqrt{\pi z^3}}(\exp(-B_1 z) - \exp(-B_2 z))\theta(z), \tag{70}$$

$$\frac{1}{\sqrt{\partial_z^2 + B^2}}\delta(z) = J_0(Bz)\theta(z), \tag{71}$$

$$\frac{(\sqrt{\partial_z^2 + B^2} - \partial_z)^\nu}{\sqrt{\partial_z^2 + B^2}}\delta(z) = B^\nu J_\nu(Bz)\theta(z), \tag{72}$$

$$\left(\frac{\sqrt{\partial_z^2 + B^2} - \partial_z}{\sqrt{\partial_z^2 + B^2} + \partial_z}\right)^{n/2}\delta(z) = \frac{1}{B^n}(\sqrt{\partial_z^2 + B^2} - \partial_z)^n\delta(z) = \frac{n}{z}J_n(Bz)\theta(z), \tag{73}$$

$$\left(\frac{\alpha\partial_z - \sqrt{\partial_z^2 + B^2}}{\alpha\partial_z + \sqrt{\partial_z^2 + B^2}}\right)\delta(z) = \frac{\alpha - 1}{\alpha + 1}\delta(z) + Bf(\alpha, Bz)\theta(z), \tag{74}$$

$$f(\alpha, z) = -\frac{8\alpha}{\alpha^2 - 1}\sum_{n=1}^{\infty} n\left(\frac{\alpha - 1}{\alpha + 1}\right)^n \frac{J_{2n}(z)}{z}, \tag{75}$$

$$\frac{\exp(-\sqrt{\partial_z^2 + B^2}a)}{\sqrt{\partial_z^2 + B^2}(\sqrt{\partial_z^2 + B^2} + \partial_z)^\nu}\delta(z) = \frac{1}{B^\nu}\left(\frac{z - a}{z + a}\right)^{\nu/2} J_\nu(B\sqrt{z^2 - a^2})\theta(z - a), \tag{76}$$

$$\begin{aligned}&\frac{\exp(-\sqrt{\partial_z^2 - B^2}a)}{\sqrt{\partial_z^2 - B^2}}\left(\frac{\partial_z - \sqrt{\partial_z^2 - B^2}}{\partial_z + \sqrt{\partial_z^2 - B^2}}\right)^\nu \delta(z)\\ &= \left(\frac{z-a}{z+a}\right)^\nu I_{2\nu}(B\sqrt{z^2 - a^2})\theta(z - a).\end{aligned} \tag{77}$$

References

1. Lindell I.V. (1993) Application of the image concept in electromagnetism. in The Review of Radio Science 1990-1992, W. Ross Stone, ed. Oxford University Press, 107–126.
2. Lindell I.V. (1995) Methods for Electromagnetic Field Analysis, 2nd ed. Oxford University Press and IEEE Press.
3. Thomson W (1872) Reprint of Papers on Electrostatics and Magnetism. Macmillan, London, pp.85, 144.
4. Heaviside O (1925) Electromagnetic Theory, Volumes I, II, III. Ernest Benn Ltd., London, second reprint.
5. van der Pol B., Bremmer H. (1959) Operational Calculus Based on the Two-Sided Laplace Integral. 2nd. ed., Cambridge University Press.
6. Mikusinski J (1959) Operational Calculus. Pergamon Press, Warsaw.
7. Lindell I.V., Valtonen M.E., Sihvola A.H. (1994) Theory of nonreciprocal and nonsymmetric uniform transmission lines. IEEE Trans. Microwave Theory Tech., **42**, 291-297.
8. Lindell I.V. (1997) Heaviside operational calculus in electromagnetic image theory. J. Electro. Waves Appl., **11**, 119–132.
9. Lindell I.V., Alanen E. (1984) Exact image theory for the Sommerfeld half-space problem, Part I: Vertical magnetic dipole. IEEE Trans. Antennas Propagat., **32**, 126–133; Part II: Vertical electric dipole, 841–847; Part III: General formulation, 1027–1032.
10. Beckmann P., Spizzichino A. (1963) The Scattering of Electromagnetic Waves from Rough Surfaces. Pergamon Press, Oxford.
11. DeSanto J.A. (1992) Scalar Wave Theory, Green's Functions and Applications. Springer, Berlin, 97–99.
12. Lindell I.V., Heiska K (1997) Simple image theory for the rough interface of two isotropic media. Microwave Opt. Tech. Lett., **14**, 333-337.
13. Lindell I.V., Alanen E., Hujanen A.T. (1987) Exact image theory for the analysis of microstrip structures. J. Electro. Waves Appl., **1**, 95–108.
14. Lindell I.V. (1988) Exact image theory for the slab problem. J. Electro. Waves Appl., **2**, 195–219.
15. Lindell I.V., Sihvola A.H., Viitanen A.J. (1990) Exact image theory for uniaxially anistropic dielectric half space. J. Electro. Waves Appl., **4**, 129–143.
16. Lindell I.V., Nikoskinen K.I., Viljanen A. (1997) Electrostatic image method for the anisotropic half space. IEE Proc. Sci. Meas. Technol., **144** 156–162.
17. Nikoskinen K.I., Lindell I.V. (1990) Time-domain analysis of the Sommerfeld VMD problem based on the exact image theory. IEEE Trans. Antennas propag., **38**, 241-250.
18. Lindell I.V. (1996) Exact image theory for vertical electromagnetic sources above a chiral half space. J. Electro. Waves Applic., **10**, 1583–1594.
19. Lindell I.V. (1992) Electrostatic image theory for the dielectric sphere. Radio Sci. **27** 1–8.
20. Lindell I.V., Ermutlu M.E., Sihvola A.H. (1992) Electrostatic image theory for layered dielectric sphere. IEE Proc. **H139** 186–192.
21. Lindell I.V., Sten J.C-E., Kleinman R.F. (1994) Low-frequency image theory for the dielectric sphere. J. Electro. Waves Appl., **8**, 295–313.

22. Lindell I.V., Ermutlu M.E., Nikoskinen K.I. (1993) Two-dimensional image theory for the conducting wedge. J. Electro. Waves Appl. **7** 179–196.
23. Ermutlu M.E., Lindell I.V., Nikoskinen K.I. (1993) Two-dimensional image theory for the conducting half plane. J. Electro. Waves Appl., **7** 971–986.
24. Nikoskinen K.I., Lindell I.V. (1995) Image solution for Poisson's equation in wedge geometry. IEEE Trans. Antennas Propag., **43**, 179–187.
25. Sten J.C-E., Lindell I.V. (1995) An electrostatic image solution for the conducting prolate spheroid. J. Electro. Waves Appl., **9**, 599-609.
26. Lindell I.V., Sihvola A.H., Muinonen K.O., Barber P.W. (1991) Scattering by a small object close to an interface, I. Exact image theory formulation. JOSA **A8**, 472–476.
27. Muinonen K.O., Sihvola A.H., Lindell I.V., Lumme K.A. (1991) Scattering by a small object close to an interface, II. Study of backscattering. JOSA **A8**, 477–482.
28. Ermutlu M.E., Muinonen K.O., Lumme K.A., Lindell I.V., Sihvola A.H. (1995) Scattering by a small object close to an interface, III. Buried object. JOSA **A12**, 1310–1315.
29. Abramowitz M., Stegun I. (1964) Handbook of Mathematical Functions. Dover, New York.